Suppression of Human Bone Morphogenetic Protein Signaling by Carboxylated Single-Walled Carbon Nanotubes

Qingxin Mu,[†,‡] Guoqing Du,[†] Taosheng Chen,[†] Bin Zhang,[‡] and Bing Yan[†,‡,*]

[†]St. Jude Children's Research Hospital, Memphis, Tennessee 38105 and [‡]Shandong University, Jinan, China

ABSTRACT Effects of carbon nanotubes (CNTs) on living systems such as cells are crucial for the safe development of biosensors, drug carriers, or tumor imaging agents. We report here that SWCNT-COOH inhibited cell proliferation *via* a nonapoptotic mechanism, which is different from effects caused by pristine CNTs. On the basis of SWCNT-COOH's perturbations on cells, expression of genes and protein, and protein phosphorylations, we conclude that SWCNT-COOH suppresses Smad-dependent bone morphogenetic protein (BMP) signaling pathway and down-regulates Id proteins. These molecular events cause cell cycle arrest at G_1/S transition and inhibit cell proliferation. The specific suppression of BMP signaling and Id proteins by SWCNT-COOH demonstrates nonapoptotic effects of functionalized CNTs on human cells. This finding may have potential therapeutic applications to treat human diseases related to Id proteins or BMP signaling such as breast cancer and bone diseases.

KEYWORDS: carbon nanotubes · BMP · TGF-β · *Id* genes · nanotoxicity · RT-CES

Mechanistic understanding of interactions between nanoparticles (NPs) and living systems has become imperative owing to the growing nanomedicine applications and the mounting societal concerns on nanosafety.[1−7] Among all NPs, carbon nanotube (CNT) has recently become a research focus because of its cancer killing and drug delivery capabilities.[8,9] Carboxylated single-walled carbon nanotubes (SWCNT-COOH) have an improved solubility profile and were used for many biological applications such as biosensors and transporters.[10,11] However, its biological effects have not yet been understood. Since water-soluble CNTs will be more likely to be used in biomedical applications, the investigation and elucidation of their cellular effects and the associated molecular mechanisms are urgently needed.

Cells maintain their homeostasis through a comprehensive signaling network.[12,13] Any perturbation of this system by nanoparticles will influence cell function and behavior. Pristine single- and multiwalled carbon nanotubes (SWCNT and MWCNT), have been shown to generate reactive oxygen species (ROS) and cause cell apoptosis *via* NF-κB signaling pathway.[2] In this study, we report that water-soluble carboxylated SWCNTs (SWCNT-COOHs, Figure 1A) inhibit cell proliferation by a nonapoptotic mechanism. By suppressing bone morphogenetic protein (BMP) signaling pathway, followed by inhibition of the expression of inhibitor of differentiation or DNA binding (Id) proteins, SWCNT-COOH caused the arrest of the cell cycle at G1/S transition and inhibited cell proliferation.

RESULTS AND DISCUSSION

SWCNT-COOH Inhibit Cell Growth through Regulating Cell Cycle without Inducing Apoptosis. When administrated in human blood circulation, soluble CNTs were excreted mainly through the urinary system.[14,15] On the basis of this consideration, we first measured the human embryonic kidney cell's response to SWCNT-COOH (Figure 2A) in real time using a real-time cell electronic sensing assay (RT-CES).[16] SWCNT-COOH is water-soluble and also well dispersed in cell culture medium (Figure 1B, insert). As shown in Figure 2A, SWCNT-COOH (100 μg/mL) triggered a sharp decrease in cell proliferation reflected by cell index (CI) within the first hour followed by a slow growth inhibition over 40 h. The conventional cell proliferation assay was also carried out and the results at different times (Figure 2B) confirmed a sudden slow-down in cell growth relative to the control at early times and a slow recovery in cell numbers afterward. This trend is similar to RT-CES assay results (Figure 2A). Morphological observation by light microscopy (Supporting Information,

*Address correspondence to bing.yan@stjude.org.

Received for review March 12, 2009 and accepted April 21, 2009.

Published online April 29, 2009.
10.1021/nn900252j CCC: $40.75

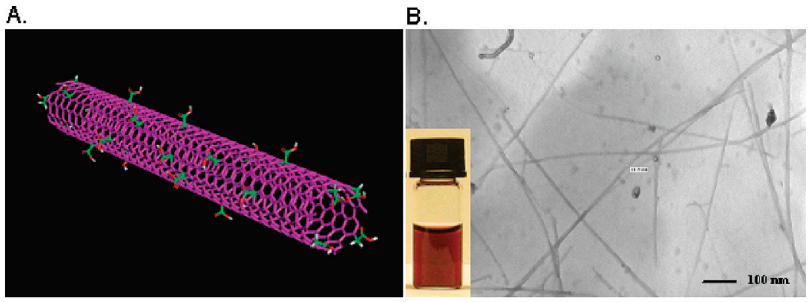

Figure 1. (A) 3-D model of SWCNT-COOH. (B) Transmission electron micrograph (TEM) of SWCNT-COOH (Scale bar, 100 nm) and photograph of SWCNT-COOH suspended in cell culture medium (insert).

Figure S1) showed the reduced cell numbers relative to the control at early times and a slow recovery afterward.

To determine whether SWCNT-COOH induced apoptotic cell death, we measured nanotube-induced DNA damage, which is a main feature of apoptosis. Using terminal deoxynucleotidyl transferase dUTP nick end labeling assay (TUNEL) on cells, we found that SWCNT-COOH did not induce apoptosis in cells (Figure 2C). In a previous report, pristine MWCNT induced DNA damage in mouse embryonic stem cells.[4] Pristine SWCNTs and MWCNTs both induced cell apoptosis *via* an activation of NF-κB signaling pathway.[2] Our results showed that soluble CNTs had a different impact on cells. To substantiate this finding, we carried out the real-time PCR analysis of 84 apoptosis-related genes using SuperArray. Results showed no significant changes in these genes (Supporting Information, Figure S2). The micrographs (Supporting Information, Figure S1) also showed no typical apoptotic phenotype after SWCNT-COOH treatment. From these results we conclude that SWCNT-COOH did not induce cell apoptosis.

We next analyzed the effect of SWCNT-COOH on cell cycle by flow cytometry (Figure 2D). The number of cells at S phase continued to decline relative to the control from 5 to 48 h after SWCNT-COOH addition. The number of cells at G2/M phase was dropped quickly in the first few hours and it gradually recovered to the normal level at 48 h. However, cells at G_0/G_1 phase showed an arrest at a level 20% higher than control cells. Our results demonstrated that water-soluble SWCNT-COOH inhibited cell growth by cell cycle arrest at G1/S transition. Therefore, cellular signaling network must be perturbed by SWCNT-COOH.

Effects on cellular signaling pathways can occur when nanotubes interact with cell surface receptors or with intracellular proteins. The evaluation of cell uptake and intracellular location of SWCNT-COOH are crucial for mechanistic understanding of its biological impact. Images from both transmission electron microscopy (TEM) (Figure 3A) and confocal laser scanning microscopy (CLSM, Figure 3B) indicated that SWCNT-COOH were translocated into cytoplasmic vesicles (Arrows in Figure 3A) within an hour. There was no evidence that SWCNT-COOH were in the nucleus. Therefore, nanotubes might interact with proteins located on cell membrane or in the cytoplasm. Furthermore, the identification of these CNT-containing endosome-like vesicles also suggested the endocytosis as a possible cell-uptake mechanism.[10]

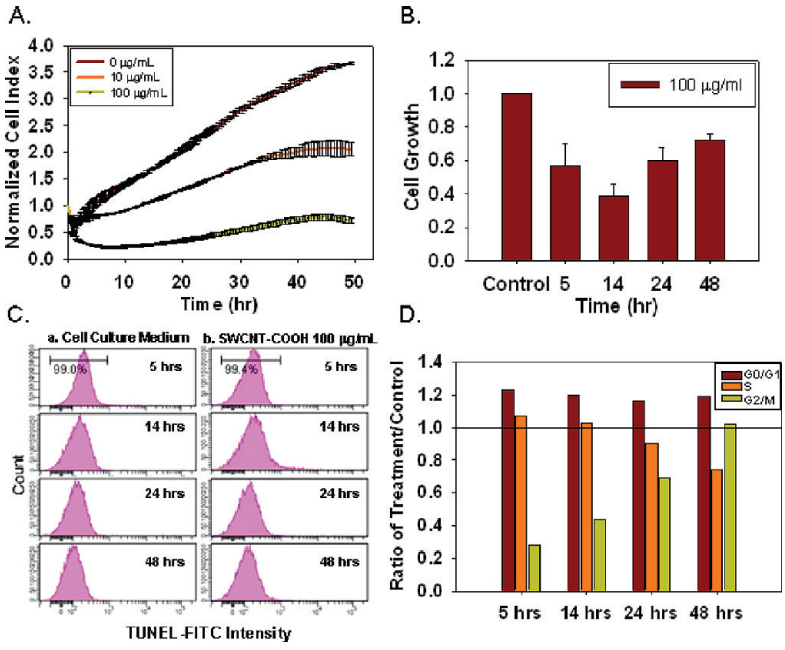

Figure 2. (A) Dynamic cellular response curves of HEK293 cells to SWCNT-COOH at various concentrations monitored by RT-CES. Error bars result from three independent measurements. (B) Cell growth ratio to control cells at different times. (C) Assessment of later phase apoptosis after addition of SWCNT-COOH (100 μg/mL) using TUNEL assay at four time points. (D) Time-dependent cell cycle regulation after addition of SWCNT-COOH (100 μg/mL).

SWCNT-COOH Down-Regulate *Id* Genes through Globe Gene Evaluation. To understand what molecular events were involved in SWCNT-COOH induced time-dependent cell growth inhibition and cell cycle regulation, we surveyed the globe gene expression profile of cells treated with SWCNT-COOH at 14 and 48 h using Affymetrix human genome U133v2 microarray that contains 54600 probesets. Gene ontology analyses of the top 10 affected biological processes indicated that the most affected biological processes are related to cell transcription besides metabolism (Table 1). Notably, TGF-β/BMP family signaling was one of the signaling pathways affected most at both time points (Supporting In-

formation, Table S1). The persistent alterations of these processes and signaling pathways might contribute to the sustained inhibition of cell proliferation.[13]

Among the 283 down-regulated genes at 14 h, 275 of them returned to normal at 48 h (Figure 4A,B). Only five genes (*Id1*, *Id2*, *Id2B*, *Id3*, and *cDNA DKFZp434L201*) remained down-regulated at both time points (Supporting Information, Table S2). Four of these five most affected genes are *Id* genes, which encode the Id proteins: Id1, Id2, and Id3. PCR experiments confirmed that *Id1* gene was significantly down-regulated after SWCNT-COOH treatment (Figure 4C) and this down-regulation was dose-dependent (Figure 4D). *Id2* and *Id3* were also down-regulated at 48 h (Figure 4C). The Id proteins are dominant-negative basic helix−loop−helix (bHLH) protein inhibitors and inhibit transcriptional activation ability of bHLH proteins.[17] Previous research has shown that Id proteins bind to pRB and release its inhibition to G1/S transition in the cell cycle.[18] The robust down-regulation of Id proteins would inhibit cell proliferation through the cell cycle arrest at G_1 to S transition.

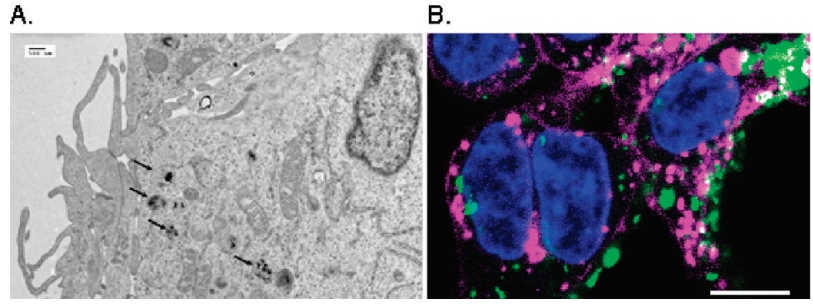

Figure 3. Cell uptake of SWCNT-COOH as shown by TEM and CLSM imaging. Both images show the uptake of SWCNT-COOH by HEK293 cells at one hour after exposure. (A) In this TEM photograph, arrows indicate SWCNT-COOHs in endosomes. The scale bar is 500 nm. (B) (Green) SWCNT-COOH labeled by FITC-BSA; (pink) cell membrane and Golgi apparatus; (blue) nucleus. Scale bar is 10 μm.

SWCNT-COOH Suppress Smad-Dependent BMP Signaling Transduction. *Id* genes are known to be the direct targets of bone morphogenetic protein (BMP) signaling pathway, which belongs to the TGF-β family.[19] In endothelial and epithelial cells, *Id* genes transcription is activated by BMP receptor signaling through Smad-dependent pathways.[20] To demonstrate the suppression of BMP signaling pathway, we investigated the inhibition of phosphorylation and expression levels of key proteins involved in this pathway such as Smad and Id proteins. Western blotting results showed that phosphoralytion of receptor Smad proteins (R-Smad or Smad1, 5, and 8) was significantly inhibited by SWCNT-COOH. At the same time, the expression of the BMP pathway targeted protein, Id1, was significantly reduced (Figure 5A).

Phosphorylated Smad proteins translocate into nucleus, bind promoters of target genes, and regulate the transcription. The inhibition of the phosphorylation by SWCNT-COOH may cause a decrease in nucleus translocation. To further prove the role of SWCNT-COOH in the inhibition of Smad1-dependent BMP signaling pathway suppression, we transfected HEK293 cells with pEGFP-Smad1 plasmid and studied the inhibition of Smad1 translocation into nucleus by SWCNT-COOH. Figure 5B shows that BMP4 activated the signaling pathway which resulted in the enhancement of Smad1 nucleus translocation (Figure 5Bb). However, the pretreatment of

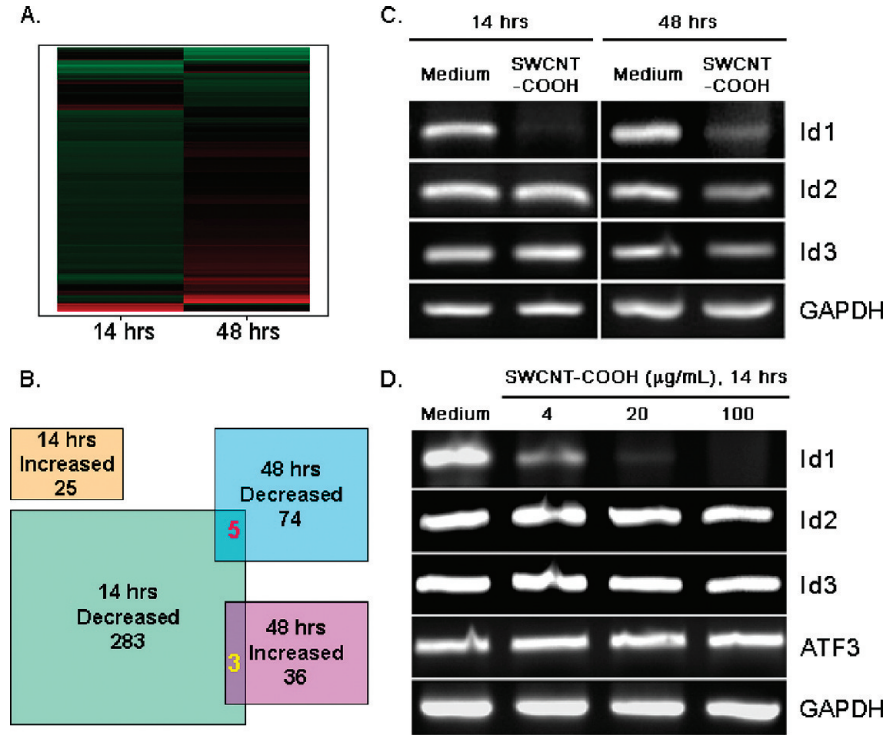

Figure 4. Gene regulation by SWCNT-COOH. (A) Heat map of 410 genes up- and down-regulated by 2-fold or more at 14 and 48 h in SWCNT-COOH treated cells as compared to the control. Expression levels: red, higher; shaded, intermediate; green, lower. (B) Number of genes whose expression levels were significantly changed after treatment with SWCNT-COOH (100 μg/mL). (C) PCR was performed to evaluate expression of *Id1*, *Id2*, and *Id3* after HEK293 cells incubated with 100 μg/mL SWCNT-COOH for 14 and 48 h, respectively. (D) Gene expression of *Id1*, *Id2*, *Id3*, and *ATF3* after HEK293 cells incubated with SWCNT-COOH for 14 h at different doses.

TABLE 1. Most Over-represented Gene Ontological Terms at 14 h and 48 h (Top 10)

14 h treatment		48 h treatment	
GO term	*p*	GO term	*p*
negative regulation of transcription factor activity	0.0000	negative regulation of transcription factor activity	0.0000
regulation of transcription factor activity	0.0000	regulation of transcription factor activity	0.0000
primary metabolism	0.0001	negative regulation of cellular metabolism	0.0003
negative regulation of transcription	0.0004	negative regulation of metabolism	0.0006
negative regulation of nucleobase, nucleoside, nucleotide and nucleic acid metabolism	0.0007	negative regulation of transcription	0.0008
regulation of metabolism	0.0013	negative regulation of nucleobase, nucleoside, nucleotide and nucleic acid metabolism	0.0011
transcription	0.0020	B cell differentiation	0.0021
negative regulation of cellular metabolism	0.0021	regulation of ligase activity	0.0041
regulation of cellular metabolism	0.0022	positive regulation of ligase activity	0.0041
regulation of transcription	0.0028	negative regulation of cellular physiological process	0.0061

cells with SWCNT-COOH blocked the process (Figure 5Bc). Our data strongly supported that Smad1-dependent BMP signaling was suppressed by SWCNT-COOH.

Besides being the direct target of Smad-dependent BMP signaling pathway, *Id* genes are also inhibited by TGF-β receptor signaling in epithelial cells through the activation of the human activating transcription factor 3 (ATF3).[21] So it is necessary to test whether SWCNT-COOH enhanced the activity of TGF-β signaling pathway. To determine the role of TGF-β pathway, we analyzed the level of *ATF3* gene. Treatment of cells with SWCNT-COOH for 14 h did not change the expression level of *ATF3* gene (Figure 4D), indicating that TGF-β receptor signaling was not activated by SWCNT-COOH.

Figure 5C proposes a plausible mechanism for SWCNT-COOH's nonapoptotic effects on cells. The inhibition of cell proliferation was triggered within 1 h according to the real-time assay and the SWCNT-COOH's cell uptake occurred also in this time frame. SWCNT-COOHs likely suppress the BMP signaling pathway by interacting with proteins, such as BMP receptors, at the cell membrane or in the cytoplasm, such as the inhibition of R-Smad phosphorylation. As a result, expression of Id1 protein was inhibited. This event results in a suppressed G1 to S transition in the cell cycle and the inhibition of cell proliferation.[17] To the best of our knowledge, similar nanostructure-induced nonapoptotic toxicity or BMP-suppression has not been reported. This suggests that more efforts need to be devoted to the study of nanoparticle's effects on signaling transduction pathways.

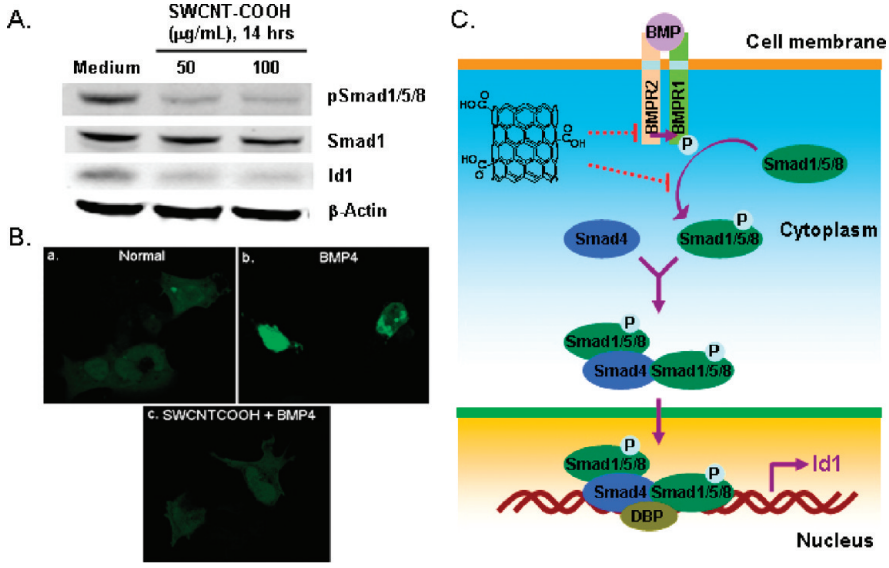

Figure 5. Suppression of BMP signaling by SWCNT-COOH. (A) Western blotting was performed to evaluate phosphoralytion level of Smad1/5/8 and expression level of Smad1, Id1, and β-actin in C33A cells after incubating with SWCNT-COOH for 14 h at 50 and 100 μg/mL, respectively. (B) SWCNT-COOH inhibit BMP4 activated nuclear translocation of Smad1. Smad1-GFP was transfected into cells: (a) normal cells; (b) cells incubated with BMP4 (50 ng/mL) for 2 h; (c) cells were pretreated with SWCNT-COOH (100 μg/mL) for 12 h before BMP4 addition. (C) Plausible mechanism for inhibition of BMP signaling by SWCNT-COOH.

CONCLUSION

In summary, SWCNT-COOH inhibited cell proliferation *via* a nonapoptotic mechanism, which is drastically different from effects caused by pristine CNTs. On the basis of SWCNT-COOH's perturbations on cells, the expression of genes and proteins, and protein phosphorylations, we conclude that SWCNT-COOH suppresses Smad-dependent BMP signaling pathway and downregulates Id proteins. These events cause cell cycle arrest at G_1/S transition and inhibit cell proliferation. The suppression of BMP signaling and Id proteins by SWCNT-COOH demonstrated nonapoptotic effects of functional-

ized CNTs on human cells. This finding may also have potential therapeutic applications in the treatment of human diseases related to Id proteins and BMP signaling, such as breast cancer[22] and bone diseases.[23]

MATERIALS AND METHODS

Cell Cultures and Reagents. SWCNT-COOHs were purchased from Sigma Aldrich (St. Louis, MO) (dimensions: 1.4∼1.6 nm (diameter) and 0.5∼1.5 μm (length); zeta potential: −63.5 mV in H_2O (pH7.0) and −12.2 mV in cell culture medium (pH 7.2∼7.4)). HEK293 (human embryonic kidney epithelial) and C33A (human cervical carcinoma epithelial) cells (from ATCC) were grown in Dulbecco's Minimum Essential Medium (DMEM, Gibco, Grand Island, NY) supplemented with 10% heat-inactivated fetal bovine serum (Invitrogen, Carlsbad, CA), 2 mM L-glutamine, 100 μg/mL penicillin, and 100 U/mL streptomycin. Guava ViaCount reagent (Guava Technologies, Hayward, CA) was used for proliferation assay. APO-BrdU Apoptosis Detection Kit was purchased from BD Biosciences (San Jose, CA). FITC-BSA was purchased from Sigma Aldrich (St. Louis, MO). Propidium iodide (Sigma Aldrich, St. Louis, MO) and RNaseA (Invitrogen, Carlsbad, CA) were used in cell cycle analysis. RNeasy Mini Kit was purchased from Qiagen (Germantown, MD). M-PER Mammalian Protein Extraction Reagent (Thermo Scientific, Franklin, MA) supplied with Halt proteases inhibitor cocktail (Thermo Scientific, Franklin, MA) was used for protein extraction. Antibodies: phosphorylated Smad1/5/8, Smad1 and Id1 (Cell Signaling, Danvers, MA); β-actin (Sigma Aldrich, St. Louis, MO). Lipofectamine 2000 transfection reagent (Invitrogen, Carlsbad, CA) was used for transfection of pEGFP-Smad1.

Real-Time Cell-Based Electronic Sensing (RT-CES) Assay. The RT-CES (ACEA Biosciences, San Diego, CA) was used for monitoring of dynamic cell growth. The cell index (CI) is derived from the cell status-based cell-electrode impedance. The cells were allowed to attach and spread on the sensor. SWCNT-COOH suspensions were added to each well when the CI reached ∼1.0. The data points were collected automatically every 15 min. Each concentration was triplicated.

Cell Growth. Cell growth ratio was monitored through live cell counting. Nanotube suspensions were added to wells 24 h after HEK293 cells seeded. The final concentration of nanotubes was 100 μg/mL. Only cell culture medium was added to control cells. After 5, 14, 24, and 48 h, cells were harvested and labeled with Guava ViaCount reagent which differentially stained viable and nonviable cells based on their permeability to DNA-binding dyes in the reagent. Viable and dead cell populations were analyzed using Guava Easycyte Minisystem with Guava Cytosoft software (Guava Technologies, Hayward, CA). Viable cells were normalized with control and plotted. Each measurement was duplicated.

TUNEL Assay. An APO-BrdU Apoptosis Detection Kit was used for labeling of the ends of DNA fragments. HEK293 cells were collected after trypsin treatment, fixed with 1% paraformaldehyde/PBS, and processed following manufacture's protocol. The labeled cells were analyzed using a BD LSR II flow cytometer (BD Biosciences, San Jose, CA).

Cell Cycle Analysis. HEK293 cells were collected after trypsin treatment, stained with propidium iodide and RNaseA, followed by analyses using BD LSR II flow cytometer. Cell cycle distribution was analyzed using ModFit LT software (Verity Software House, Topsham, ME).

Transmission Electron Microscopy (TEM). HEK293 cells were treated with 100 μg/mL for 1 h. Then cells were fixed in 2.5% glutaraldehyde in 0.1 M sodium cacodylate buffer (pH 7.4) and rinsed. Cells were then post fixed 1 h in 2% osmium tetroxide with 3% potassium ferriocyanide and rinsed, and then enbloc stained with a 2% aqueous uranyl acetate solution and dehydration through a graded series of alcohol. They were then put into two changes of propylene oxide, a series of propylene/Epon dilutions, and embedded. The thin (70 μm) sections were cut on a Leica UC6 ultramicrotome and images were taken on a JEOL 1200 EX (JEOL, Ltd. Tokyo, Japan) using an AMT 2k digital camera.

Confocal Laser Scanning Microscopy (CLSM). FITC-BSA and SWCNT-COOH were incubated at 4 °C overnight. Free FITC-BSA was removed through centrifuge (16000*g*, 30 min) and washing. SWCNT-COOH/FITC-BSAs were resuspended in deionized water; HEK293 cells were incubated with SWCNT-COOH/FITC-BSA for 1 h. Cells were then fixed with 4% paraformaldehyde (PFA) and stained with 10 μg/mL WGA-Alexa Fluor 647 (Invitrogen, Carlsbad, CA). Then cells were mounted with VECTASHIELD mounting medium (with DAPI) (Vector Laboratories, Inc. Burlingame, CA) at 4 °C overnight. The images were analyzed using laser scanning microscope LSM 510, version 3.2 SP2 (Carl Zeiss GmbH, Germany).

Microarray Analysis. Total RNA was extracted from HEK293 cells using RNeasy Mini Kit, and RNA integrity was assessed accoding to manufacture's protocol. The Affymetrix U133 plus 2.0 GeneChip array (Affymetrix, Inc. Santa Clara, CA) was used to determine expression data. The relative expression signals for each gene were calculated using MicroArray Suite version 5.0 (MAS5.0; Affymetrix, Inc. Santa Clara, CA). The generation of heat map of significant affected genes and gene ontology analyses were performed using the software package Spotfire DecisionSite 7.0 (Spotfire Inc. Somerville, MA).

Reverse Transcription PCR. RNA samples extracted from HEK293 on microarray analysis were used for PCR analysis. PCR primers were used as following sequences:

*Id1*5′-AGCCAGTCCGCCAAGAATCAT-3′ (forward),
5′-ACTCACTCCCCAGCATGAAG-3′ (reverse);
*Id2*5′-ACGACCCGATGAGCCTGCTA-3′ (forward),
5′-TCCTGGAGCGCTGGTTCTG-3′ (reverse);
*Id3*5′-CTCCACGCTCTGAAAAGACC-3′ (forward),
5′-ACTCAGATTAAGCCAGGTGGA-3′ (reverse);
*ATF3*5′- CTGGGTCACTGGTGTTTGAG-3′ (forward),
5′- CGCTGACAGTGACTGATTCC −3′ (reverse);
*GAPDH*5′-ATCACTGCCACCCAGAAGAC-3′ (forward),
5′-ATGAGGTCCACCACCCTGTT-3′ (reverse).

Target genes were amplified and PCR products were loaded onto 2% agarose gels and run at 80 V for 1 h.

Western Blotting. C33A cells were washed with ice cold PBS ×3 and collected through scratching and centrifugation. Cells were lysed using M-PER mammalian protein extraction reagent supplied with Halt proteases inhibitor cocktail and protein concentrations were determined using the NanoDrop spectrophotometer (Thermo Scientific, Franklin, MA). Equal amounts of proteins were loaded on NuPAGE gradient Bis-Tris gels (4%∼12%) (Invitrogen, Carlsbad, CA) and transferred onto nitrocellulose membrane using iBlot dry blotting system (Invitrogen, Carlsbad, CA). Membranes were blocked for 2 h with Odyssey blocking buffer (LI-COR Biotechnology, Lincoln, NB) at room temperatures followed by incubation overnight at 4 °C with antibodies against phosphorylated Smad1/5/8, Smad1, Id1, and β-actin. Membranes were washed in PBST (PBS with 0.1% Tween-20) and incubated for 1 h with IRDye 800CW labeled secondary antibodies (LI-COR Biotechnology, Lincoln, NB). Visualization was performed using Odyssey System (LI-COR Biotechnology, Lincoln, NB).

Nuclear Translocation of Smad1. HEK293 cells were stably transfected with pEGFP-Smad1 using Lipofactamine reagent according to manufacture's protocol. Briefly, cells were seeded in 24-well plates at the density of 100000/well. pDNA and liposome (1:2.5 m/v) were mixed and incubated for 5 min before adding into cells. Complex was removed 6 h after addition and replaced with normal medium. After 24 h culture, cells were replaced with DMEM (10% FBS, 800 μg/mL G418) selective medium and cultured for 2 weeks prior to experiment. Cells were subsequently seeded into 3 glass bottom culture dishes. One dish was added with SWCNT-COOH 100 μg/mL for 12 h followed by BMP4 50 ng/mL treated for 2 h. Another one was treated with

BMP4 50 ng/mL for 2 h only. The last one was used as normal control. Cells were then fixed with 4% paraformaldehyde and mounted with PPD mounting medium and imaged using CLSM.

Acknowledgment. We thank Ms. Sharon Frase (St. Jude Children's Research Hospital) for acquiring transmission electron images. We thank Dr. Fu-yue Zeng and Dr. Haotian Zhao (St. Jude Children's Research Hospital) for research discussions. We also thank Prof. Craig Robson (Newcastle University, United Kingdom) for providing pEGFP-Smad1 plasmid. This work was supported by the American Lebanese Syrian Associated Charities (ALSAC), St. Jude Children's Research Hospital, and the National Basic Research Program of China (973 Program 2009CB930103).

Supporting Information Available: Morphological observation by light microscope, real-time PCR of apoptosis genes by superarray, signaling pathways significantly affected and fold changes of *Id* genes by microarray analysis. This material is available free of charge *via* the Internet at http://pubs.acs.org.

REFERENCES AND NOTES

1. Ding, L. H.; Stilwell, J.; Zhang, T. T.; Elboudwarej, O.; Jiang, H. J.; Selegue, J. P.; Cooke, P. A.; Gray, J. W.; Chen, F. Q. F. Molecular Characterization of the Cytotoxic Mechanism of Multiwall Carbon Nanotubes and Nano-onions on Human Skin Fibroblast. *Nano Lett.* **2005**, *5*, 2448–2464.
2. Manna, S. K.; Sarkar, S.; Barr, J.; Wise, K.; Barrera, E. V.; Jejelowo, O.; Rice-Ficht, A. C.; Ramesh, G. T. Single-Walled Carbon Nanotube Induces Oxidative Stress and Activates Nuclear Transcription Factor kappa B in Human Keratinocytes. *Nano Lett.* **2005**, *5*, 1676–1684.
3. Zhang, T. T.; Stilwell, J. L.; Gerion, D.; Ding, L. H.; Elboudwarej, O.; Cooke, P. A.; Gray, J. W.; Alivisatos, A. P.; Chen, F. F. Cellular Effect of High Doses of Silica-Coated Quantum Dot Profiled with High Throughput Gene Expression Analysis and High Content Cellomics Measurements. *Nano Lett.* **2006**, *6*, 800–808.
4. Zhu, L.; Chang, D. W.; Dai, L. M.; Hong, Y. L. DNA Damage Induced by Multiwalled Carbon Nanotubes in Mouse Embryonic Stem Cells. *Nano Lett.* **2007**, *7*, 3592–3597.
5. Chou, C. C.; Hsiao, H. Y.; Hong, Q. S.; Chen, C. H.; Peng, Y. W.; Chen, H. W.; Yang, P. C. Single-Walled Carbon Nanotubes Can Induce Pulmonary Injury in Mouse Model. *Nano Lett.* **2008**, *8*, 437–445.
6. Zhou, H.; Mu, Q.; Gao, N.; Liu, A.; Xing, Y.; Gao, S.; Zhang, Q.; Qu, G.; Chen, Y.; Liu, G.; Zhang, B.; Yan, B. A Nano-Combinatorial Library Strategy for the Discovery of Nanotubes with Reduced Protein-Binding, Cytotoxicity, and Immune Response. *Nano Lett.* **2008**, *8*, 859–865.
7. Mu, Q.; Li, Z.; Li, X.; Mishra, S. R.; Zhang, B.; Si, Z.; Yang, L.; Jiang, W.; Yan, B. Characterization of Protein Clusters of Diverse Magnetic Nanoparticles and Their Dynamic Interactions with Human Cells. *J. Phys. Chem. C* **2009**, *113*, 5390–5395.
8. Liu, Z.; Chen, K.; Davis, C.; Sherlock, S.; Cao, Q. Z.; Chen, X. Y.; Dai, H. J. Drug Delivery with Carbon Nanotubes for *in Vivo* Cancer Treatment. *Cancer Res.* **2008**, *68* (16), 6652–6660.
9. Chakravarty, P.; Marches, R.; Zimmerman, N. S.; Swafford, A. D. E.; Bajaj, P.; Musselman, I. H.; Pantano, P.; Draper, R. K.; Vitetta, E. S. Thermal Ablation of Tumor Cells with Anti Body-Functionalized Single-Walled Carbon Nanotubes. *Proc. Natl. Acad. Sci. U.S.A.* **2008**, *105*, 8697–8702.
10. Kam, N. W. S.; Liu, Z. A.; Dai, H. J. Carbon Nanotubes As Intracellular Transporters for Proteins and DNA: An Investigation of the Uptake Mechanism and Pathway. *Angew. Chem., Int. Ed.* **2006**, *45*, 577–581.
11. Huang, X. J.; Im, H. S.; Yarimaga, O.; Kim, J. H.; Lee, D. H.; Kim, H. S.; Choi, Y. K. Direct Electrochemistry of Uric Acid at Chemically Assembled Carboxylated Single-Walled Carbon Nanotubes Netlike Electrode. *J. Phys. Chem. B* **2006**, *110*, 21850–21856.
12. White, M. A.; Anderson, R. G. W. Signaling Networks in Living Cells. *Annu. Rev. Pharmacol. Toxicol.* **2005**, *45*, 587–603.
13. Massague, J.; Blain, S. W.; Lo, R. S. TGF Beta Signaling in Growth Control, Cancer, And Heritable Disorders. *Cell* **2000**, *103*, 295–309.
14. Cherukuri, P.; Gannon, C. J.; Leeuw, T. K.; Schmidt, H. K.; Smalley, R. E.; Curley, S. A.; Weisman, R. B. Mammalian Pharmacokinetics of Carbon Nanotubes Using Intrinsic Near-Infrared Fluorescence. *Proc. Natl. Acad. Sci. U.S.A.* **2006**, *103*, 18882–18886.
15. Singh, R.; Pantarotto, D.; Lacerda, L.; Pastorin, G.; Klumpp, C.; Prato, M.; Bianco, A.; Kostarelos, K. Tissue Biodistribution and Blood Clearance Rates of Intravenously Administered Carbon Nanotube Radiotracers. *Proc. Natl. Acad. Sci. U.S.A.* **2006**, *103* (9), 3357–3362.
16. Solly, K.; Wang, X. B.; Xu, X.; Strulovici, B.; Zheng, W. Application of Real-Time Cell Electronic Sensing (RT-CES) Technology to Cell-Based Assays. *Assay Drug Dev. Technol.* **2004**, *2*, 363–372.
17. Norton, J. D.; Deed, R. W.; Craggs, G.; Sablitzky, F. Id Helix–Loop–Helix Proteins in Cell Growth and Differentiation. *Trends Cell Biol.* **1998**, *8*, 58–65.
18. Hara, E.; Uzman, J. A.; Dimri, G. P.; Nehlin, J. O.; Testori, A.; Campisi, J. The Helix–Loop–Helix Protein Id-1 and a Retinoblastoma Protein Binding Mutant of SV40 T Antigen Synergize to Reactivate DNA Synthesis in Senescent Human Fibroblasts. *Dev. Genet.* **1996**, *18*, 161–172.
19. Hollnagel, A.; Oehlmann, V.; Heymer, J.; Ruther, U.; Nordheim, A. *Id* Genes Are Direct Targets of Bone Morphogenetic Protein Induction in Embryonic Stem Cells. *J. Biol. Chem.* **1999**, *274*, 19838–19845.
20. Korchynskyi, O.; ten Dijke, P. Identification and Functional Characterization of Distinct Critically Important Bone Morphogenetic Protein-Specific Response Elements in the Id1 Promoter. *J. Biol. Chem.* **2002**, *277*, 4883–4891.
21. Kang, Y. B.; Chen, C. R.; Massague, J. A Self-Enabling TGF Beta Response Coupled to Stress Signaling: Smad Engages Stress Response Factor ATF3 for Id1 Repression in Epithelial Cells. *Mol. Cell* **2003**, *11*, 915–926.
22. Fong, S.; Itahana, Y.; Sumida, T.; Singh, J.; Coppe, J. P.; Liu, Y.; Richards, P. C.; Bennington, J. L.; Lee, N. M.; Debs, R. J.; Desprez, P. Y. Id-1 as a Molecular Target in Therapy for Breast Cancer Cell Invasion and Metastasis. *Proc. Natl. Acad. Sci. U.S.A.* **2003**, *100*, 13543–13548.
23. Sulzbacher, I.; Birner, P.; Trieb, K.; Pichlbauer, E.; Lang, S. The Expression of Bone Morphogenetic Proteins in Osteosarcoma and Its Relevance As a Prognostic Parameter. *J. Clin. Pathol.* **2002**, *55*, 381–385.